

New Thermosets Obtained by Cationic Copolymerization of DGEBA with γ -Caprolactone with Improvement in the Shrinkage. II. Time–Temperature–Transformation (TTT) Cure Diagram

Servando González,¹ Xavier Fernández-Francos,¹ Josep Maria Salla,¹ Angels Serra,²
Ana Mantecón,² Xavier Ramis¹

¹Laboratori de Termodinàmica, ETSEIB, Universitat Politècnica de Catalunya, Diagonal 647, 08028 Barcelona, Spain

²Departament de Química Analítica i Química Orgànica, Universitat Rovira i Virgili, Marcellí Domingo s/n, 43007 Tarragona, Spain

Received 24 October 2006; accepted 7 December 2006

DOI 10.1002/app.26021

Published online 8 March 2007 in Wiley InterScience (www.interscience.wiley.com).

ABSTRACT: Mixtures of diglycidylether of bisphenol A (DGEBA) with different proportions of γ -caprolactone (γ -CL) were cured with ytterbium triflate as initiator. The curing was studied with differential scanning calorimetry (DSC) and thermo mechanical analysis (TMA). The results are presented in the form of a time–temperature–transformation diagram. The kinetic analysis was performed by means of the isoconversional integral procedure and the kinetic model was also determined using the Coats–Redfern method. Gelation was determined by means of combined experiences of DSC and TMA. The relationship between the glass transition temperature (T_g) and the degree of conver-

sion α was determined by DSC. Using the isoconversional lines and the T_g - α relationship, the vitrification curve was obtained. The methodology developed makes it possible to obtain the TTT diagram using only no-isothermal experiments with equivalent results to those using classical isothermal procedures. The addition of γ -CL accelerates the curing and reduces the shrinkage after gelation and consequently the internal stresses in the material. © 2007 Wiley Periodicals, Inc. *J Appl Polym Sci* 104: 3406–3416, 2007

Key words: epoxy networks; lactones; gelation; kinetics (polym.); time–temperature–transformation

INTRODUCTION

In the first part of this study,¹ we characterized new thermosetting materials obtained by means of copolymerization of diglycidylether of bisphenol A (DGEBA) with γ -CL using ytterbium triflate as the curing initiator. This methodology made it possible to insert ester groups and aliphatic chains into the polymer network. The aim of the insertion of these groups was to address some of the problems that arise in the applications of conventional epoxy resins, such as contraction during the curing process and low degradability at the end of their useful life. In particular, we showed that the addition of γ -CL reduces contraction after gelation and that the

materials obtained in this way are more flexible and more thermally degradable than cationic crosslinked DGEBA.

Ring-opening polymerization of heterocyclic expanding monomers without the formation of small molecules as a by-product can lead to materials that shrink little or even expand and insert weak bonds in the network.^{1–9} Spiroorthoesters (SOEs) are bicyclic compounds that are commonly used as expanding monomers and can be synthesized from lactones and epoxides under Lewis acid catalysis.^{10,11} The use of five-member lactones, which are unable to homopolymerize for thermodynamic reasons, ensures the formation of an intermediate SOE.^{4,12} As we have seen in previous studies,^{1,5,6,13–15} where different epoxy monomers were copolymerized with lactones with distinct structures, the polymerization of the SOE formed at the end of the curing process is the process that is responsible for the lower contraction after gelation. In these works, we also identified the following reactive processes that occur during the curing process: (a) homopolymerization of the DGEBA, (b) reaction between the DGEBA and the lactone giving rise to formation of the SOE, (c) DGEBA/SOE copolymerization, and (d) homopolymerization of the SOE. The impact of these reactions

Correspondence to: X. Ramis (ramis@mmt.upc.edu).

Contract grant sponsor: CYCIT (Comisión Interministerial de Ciencia y Tecnología).

Contract grant sponsor: FEDER (European Regional Development Fund); contract grant number: MAT2004-04, 165-C02-02.

Contract grant sponsor: CYCIT, FEDER; contract grant number: MAT2005-01,806.

Journal of Applied Polymer Science, Vol. 104, 3406–3416 (2007)
© 2007 Wiley Periodicals, Inc.

will depend on the composition of the mixture and on the kinetics of each of these processes. The schemes for these reaction processes for the DGEBA/ γ -CL system studied are shown in the first part of this work.¹

The complexity of the DGEBA/lactone reaction process makes it difficult to characterize the curing of these systems completely. As already mentioned, there are different chemical reactions with differing kinetics, and different physical processes also take place in curing (gelation and vitrification) that can affect not only the curing process but also the physical properties of the material.

Gelation is an isoconversional effect that corresponds to the formation of the first insoluble fraction of polymer of infinite molecular weight. From the standpoint of processing, gelation represents the point after which the material can no longer be processed and contraction gives rise to internal stresses in the gelled material. Gelation does not involve any change in the curing kinetics, so it cannot be determined directly by calorimetry. It must therefore be determined by means of techniques that measure changes in mechanical and/or viscoelastic properties, or through testing of loss of solubility.¹⁶ In this study, we present a nonisothermal methodology that combines TMA and DSC testing to determine gelation with results equivalent to testing of loss of solubility.

Vitrification is understood as the change from the liquid or rubbery state to the glassy state due to an increase in both the crosslinking density and the molecular weight of the material during the curing process. This transformation occurs when the T_g of the material coincides with the curing temperature. In this study, we determine vitrification on the basis of the T_g - α relationship of the system and the isoconversional kinetic data. The methodology used is a fast and reliable alternative to conventional determination of vitrification by means of different techniques, such as DSC,¹⁷ alternating DSC,¹⁸ torsional braid analysis,¹⁹ and dynamic mechanical thermal analysis.²⁰

The different states that the material can pass through during the curing process can be represented in time-temperature-transformation (TTT) diagrams.²¹ The TTT diagram is unique to the curing of each thermoset system and allows us to determine the optimum conditions for curing and make a tentative prediction of the final properties of the material. Construction of this diagram requires knowledge of the curing kinetics, and of when and how the material gels and vitrifies.

This work had two aims: first, we wished to gain detailed knowledge of the complex curing of the DGEBA/ γ -CL systems. To do so we established the curing kinetics by means of an integral isoconversional methodology and determined gelation and vitrification as set out above. The results will be presented, for some of the systems studied, in the form of a TTT diagram. Special emphasis will be placed on the influence of the amount of γ -CL on the curing kinetics and on the gelation of the material, as well as the potential influence of gelation on contraction. Second, we wished to establish a simple methodology for determining TTT diagrams that can be applied to any thermoset system.

EXPERIMENTAL

Materials

DGEBA, Epitoke Resin 828 from Shell Chemicals (epoxy equivalent = 187 g/eq), was used as received. γ -Caprolactone (γ -CL), (molecular mass = 114.14 g/mol, 98%) (Aldrich) and ytterbium (III) trifluoromethanesulfonate (99.99%) (Aldrich) were used as received.

Table I shows the various formulations that were used, their notation, and the proportions of the different reactants.

Preparation of the curing mixtures

Samples were prepared by adding to the corresponding mixtures of γ -CL and DGEBA 3 phr of

TABLE I
Formulations and Heat of Polymerization of the Systems Studied

Formulations ^a	Notation	Eq. initiator/eq. epoxide	Eq. initiator/eq. total	γ -CL (% w/w)	Δh^b (J/g)	Δh^c (kJ/ee)
DGEBA/ γ -CL 1 : 0	1 : 0	0.0271	0.0271	0	525	101
DGEBA/ γ -CL 3 : 1	3 : 1	0.0299	0.0256	8.1	438	93
DGEBA/ γ -CL 2 : 1	2 : 1	0.0313	0.0250	10.5	417	93
DGEBA/ γ -CL 1 : 1	1 : 1	0.0354	0.0236	15.9	387	97
DGEBA/ γ -CL 1 : 2	1 : 2	0.0437	0.0218	37.9	308	96

^a The composition of the formulation are given in molar ratios, and 3 phr of ytterbium triflate as initiator was used in all cases.

^b Enthalpies per gram of mixture.

^c Enthalpies per equivalent of epoxy group.

ytterbium triflate (3 part per 100 parts of mixture, w/w). Samples were carefully stirred and kept at -20°C before use to prevent polymerization.

DSC calorimetry

Calorimetric analyses were carried out on a Mettler DSC-822e calorimeter with a TSO801RO robotic arm. Samples of approximately 10 mg in weight were cured in aluminum pans in a nitrogen atmosphere. Nonisothermal experiments were performed between 0 and 225°C at heating rates of 2, 5, 10, and $15^{\circ}\text{C}/\text{min}$ to determine the reaction heat. In the nonisothermal curing process, the degree of conversion at a given temperature T was calculated as the quotient between the heat released up to T and the total reaction heat associated with complete conversion of all reactive groups. In a similar way, the reaction rate, $d\alpha/dt$, at a given temperature can be expressed as the quotient between the calorimetric signal at a temperature T and the total heat of reaction.

Isothermal curing was carried out for different times at temperature of 140°C . After curing, the sample was cooled and by means of a dynamic scan at $10^{\circ}\text{C}/\text{min}$, the residual heats were determined. With isothermal curing the degree of conversion was calculated on the basis of residual heat taking into account the total reaction heat.

To establish the relations T_g - α we performed a series of nonisothermal scans from 20°C to several temperatures, below 225°C , at a heating rate of $10^{\circ}\text{C}/\text{min}$. Then, the samples were immediately quenched and a second scan from -100 to 225°C at a heating rate of $10^{\circ}\text{C}/\text{min}$ was registered to determine the T_g value and the residual heat. The degree of conversion was determined in a similar way that isothermal curing. The T_g was measured as the half-way point of the jump in the heat capacity when the material changed from the glassy to the rubbery state ($\Delta C_p = C_{p(r)} - C_{p(g)}$). ΔC_p was also measured in materials uncured and completely cured.

Thermomechanical analysis (TMA)

Thermal mechanical analysis was carried out in a nitrogen atmosphere using a Mettler TMA40 thermomechanical analyzer. The samples were supported by two small circular ceramic plates and silanized glass fibers, which were impregnated with the sample. Nonisothermal experiments were performed between 40 and 225°C at heating rate of $5^{\circ}\text{C}/\text{min}$ applying a periodic force that changed (cycle time = 12 s) from 0.0025 to 0.01N. When the material reached sufficient mechanical stability (gelation) the TMA measuring probe deforms less to the sample and the amplitude of the oscillations is reduced. The gel point was taken in TMA as the temperature at

which sudden decrease in the amplitude of oscillations was observed. The gel conversion, α_{gel} , was determined as the DSC conversion at the temperature of the material gelled in TMA in a nonisothermal experiment.

KINETIC ANALYSIS

Isoconversional methodology assumes that, at a given degree of conversion, the reaction mechanism does not depend on the heating rate in nonisothermal experiments and or on the temperature of reaction in isothermal experiments.²²

Accepting that $d\alpha/dt$ depends on the temperature and the advance of the reaction and that the dependence of the rate constant on the temperature follows Arrhenius equation, the kinetic of reaction is usually described as:

$$\frac{d\alpha}{dt} = kf(\alpha) = A \exp\left(-\frac{E}{RT}\right)f(\alpha) \quad (1)$$

where k is the rate constant, A is the pre-exponential factor, E is the activation energy, R is the universal gas constant, T is the temperature and $f(\alpha)$ is a function which depends on the degree of conversion and represents the kinetic model that governs the process.

By integrating the rate equation, Eq. (1), under nonisothermal condition and using the Coats-Redfern²³ approximation to solve the so-called temperature integral and considering that $2RT/E$ is much lower than 1, the Kissinger-Akahira-Sunose (KAS) equation may be written:²⁴

$$\ln\left(\frac{\beta}{T^2}\right) = \ln\left[\frac{AR}{g(\alpha)E}\right] - \frac{E}{RT} \quad (2)$$

where β is the heating rate and $g(\alpha)$ is the integral conversion function.

For each conversion degree, the linear plot of $\ln(\beta/T^2)$ versus $1/T$ enables E and $\ln[AR/g(\alpha)E]$ to be determined from the slope and the intercept. If the reaction model, $g(\alpha)$, is known, the corresponding pre-exponential factor can be calculated for each conversion. The Flynn-Wall-Ozawa integral method²⁵ was not used because it gives equivalent results to the KAS method.

Integration of Eq. (1) in isothermal conditions gives the isoconversional expression:

$$\ln t = \ln\left[\frac{g(\alpha)}{A}\right] + \frac{E}{RT} \quad (3)$$

where t is cure time.

It can be observed how the isothermal constant $\ln[g(\alpha)/A]$ [Eq. (3)] is directly related by R/E for

every value of α to the constant $\ln[AR/g(\alpha)E]$ of the nonisothermal adjustment [Eq. (2)]. Thus, taking the nonisothermal data $\ln[AR/g(\alpha)E]$ and E from eq. (2), we can determine the isothermal parameters of Eq. (3) and simulate isothermal curing without knowing $g(\alpha)$.

Reordering eq. (2) we can write the Coats–Redfern equation:

$$\ln\left(\frac{g(\alpha)}{T^2}\right) = \ln\left[\frac{AR}{\beta E}\right] - \frac{E}{RT} \quad (4)$$

For a given kinetic model, linear plot of $\ln(g(\alpha)/T^2)$ versus $1/T$ permit us to determine E and A from the slope and the intercept.

In this work, kinetic analysis was performed with nonisothermal integral isoconversional methods [eq. (2)]. Isothermal polymerization was simulated with nonisothermal data applying eq. (3). We selected the kinetic model that had the best linear correlation in the Coats–Redfern equation [eq. (4)] and that had an E value similar to the obtained isconversionally that was taken as the effective value because was determined without knowing the kinetic model. Different kinetic models were studied: diffusion (D_1 , D_2 , D_3 , and D_4), Avrami–Erofeev ($A_{3/2}$, A_2 , A_3 , and A_4), power law (P_2), phase-boundary-controlled reaction (R_2 and R_3), reaction-order n ($n = 3, 2, 1.5$, and 1 denominated F_1) and autocatalytic ($n + m = 2$ with $n = 1.5$ and $n = 1.9$).^{26,27} Although there is no reason for some of these models to have any physicochemical meaning in the curing processes, they can still be used to describe the calorimetric curve. The kinetic methodology applied in this work has been used previously in different reactive systems with good

results.^{26–29} Although it is accepted that the use of differential methods leads to more consistent values of the activation energy than does the use of the integral methods, we used those because are easy amenable and it permits us to simulate the curing.^{29,30}

RESULTS AND DISCUSSION

First of all, we analyzed the kinetic methodology applied to the curing of the pure resin (formulation 1 : 0). This methodology was then applied to the other formulations, to determine the effect of the γ -CL on the curing kinetics.

Figure 1 shows the calorimetric curves, reaction rate and conversion (inset) against temperature, for different heating rates of the 1 : 0 formulation. It can be observed that with the increase in the heating rate the curves are shifted to higher temperatures. In general, a single process is observed with a shoulder at high temperature. This shape of the curve could be related to competition between the two mechanisms of cationic polymerization, i.e., ACE (activated chain end) and AM (activated monomer). As a rule, the use of large amounts of initiator, as in this case, would give rise to a greater number of active centers at the start of the reaction that would favor the AM mechanism over the ACE mechanism.³¹ Evidence of competition between the AM and ACE mechanisms has already been observed in epoxy and epoxy/lactone systems.^{13,31–33}

Table II shows the kinetic data obtained for the 1 : 0 formulation on the basis of the experimental curves of Figure 1. It can be observed that the activation energy rose slightly with the increase in

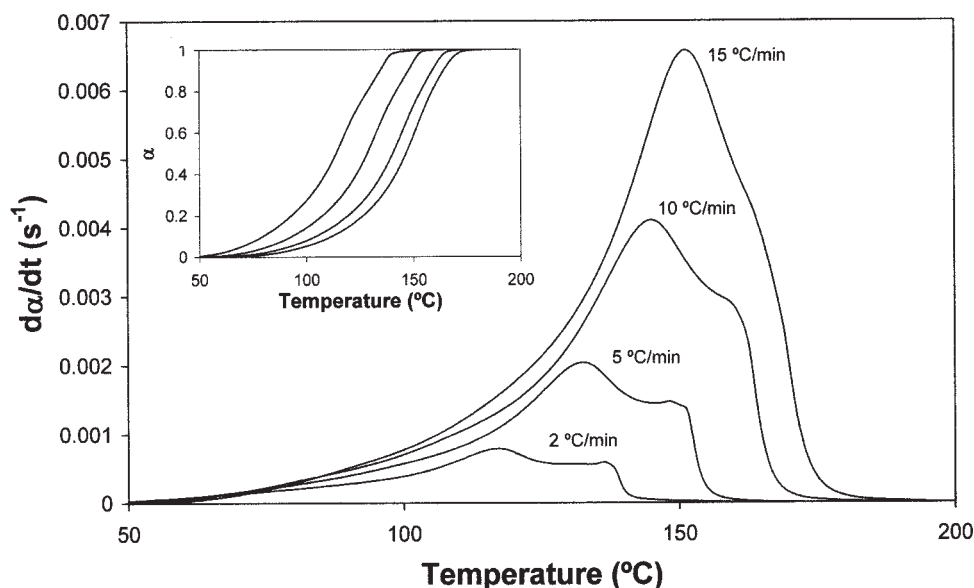


Figure 1 Rate of reaction of nonisothermal curing for DGEBA/ γ -CL 1 : 0 formulation at different heating rates (2, 5, 10, and 15 °C/min). The inset shows conversion versus the temperature at same heating rates.

TABLE II
Kinetic Parameters of Nonisothermal Polymerization for Formulation DGEBA/ γ -CL 1:0 Obtained by Eq. (2)

α	E^a (kJ/mol)	$\ln[AR/g(\alpha)E]^a$ ($K^{-1} \text{ min}^{-1}$)	$\ln[g(\alpha)/A]^b$ (min^{-1})	r^2	$\ln A^c$ (min^{-1})	$k_{140^\circ\text{C}}^d$ (min^{-1})	t_{exp}^e (min)	t_{sim}^f (min)
0.05	65.9	12.19	-21.17	0.9978	17.09	0.1219	0.15	0.14
0.1	64.6	11.01	-19.97	0.9995	16.60	0.1096	0.32	0.31
0.2	65.9	10.55	-19.53	1.0000	16.90	0.1004	0.71	0.71
0.3	68.8	10.88	-19.90	0.9999	17.71	0.0986	1.10	1.15
0.4	71.1	11.19	-20.24	0.9998	18.39	0.0984	1.45	1.59
0.5	72.7	11.38	-20.45	0.9997	18.88	0.0993	1.92	2.06
0.6	74.5	11.63	-20.73	0.9996	19.40	0.1016	2.41	2.63
0.7	78.1	12.44	-21.59	0.9993	20.48	0.1049	3.10	3.17
0.8	84.5	14.00	-23.22	0.9990	22.34	0.1045	3.87	4.01
0.9	89.8	15.17	-24.45	0.9989	23.83	0.0977	5.16	5.49
0.95	93.3	15.98	-25.31	0.9993	24.85	0.0984	6.12	6.44

^a $\ln[AR/g(\alpha)E]$ and E have been calculated on the basis of the nonisothermal DSC experiments, as the intercept and the slope of the isoconversional relationship $\ln[\beta/T^2] = \ln[AR/g(\alpha)E] - E/RT$.

^b $\ln[g(\alpha)/A]$ has been calculated on the basis of $\ln[AR/g(\alpha)E]$ and E .

^c $\ln A$ has been calculated using kinetic model R_3 and $\ln[g(\alpha)/A]$ or $\ln[AR/g(\alpha)E]$.

^d Values of rate constant at 140°C calculated using the Arrhenius equation and the values of E and $\ln A$.

^e Experimental curing times at 140°C determined by DSC.

^f Simulated curing times at 140°C determined using eq. (3) and the parameters E and $\ln[g(\alpha)/A]$.

conversion. This rise became more pronounced in the final phase of curing, coinciding with the appearance of the shoulder in the DSC curves. One possible explanation for this rise may be found in the depletion of the reactive species, the increase in the viscosity of the reaction medium and the competition between mechanisms with the increase in conversion. In many reaction processes the variations in E do not actually reflect kinetic changes, due to the compensation effect between the activation energy and the pre-exponential factor.^{22,27-29,33} To establish whether or not the curing kinetics were constant or invariable throughout the curing process, we needed to determine the kinetic model and then estimate the pre-exponential factor and the kinetic constant by means of the Arrhenius equation. The value of the rate constant, k , is a better reflection of the actual kinetic changes, since it includes both the effect of the activation energy and the pre-exponential factor. In spite of the slight variations in E , to establish the overall kinetic model governing the process we used the Coats-Redfern method between conversions of 0.1 and 0.9. Table III shows the results obtained at $10^\circ\text{C}/\text{min}$. Other heating rates gave similar results. Thanks to the linearization involved in this method, several models give a good regression. To discriminate the model correctly, we need to know the true value of E , which can be taken as the mean of the value obtained isoconversionally (Table II).^{26-30,33} For the 1 : 0 formulation (between conversions of 0.1 and 0.9), the mean of E has a value of 74.4 kJ/mol . R_3 was taken as the kinetic model because, with a good correlation coefficient, it is the one that gives an E closest to the one obtained isoconversionally (Table III). The R_2 model could also be used to

describe the curing process. Models such as D_1 , D_2 , D_3 , and D_4 were ruled out because E is not close to the true value, although they do give good correlations. Models with correct values for E (F_1 , $n = 1.5$) were also ruled out, since their correlations are low.

Having established the R_3 model on the basis of the isoconversional parameters, we determined A and the kinetic constant at a reference temperature of 140°C (Table II). The very small variation found in k during the curing process indicates that the kinetic changes are of little importance. It was also observed that the values of E and $\ln A$ can be related to a good correlation by means of an isokinetic relationship (IKR) with an isokinetic temperature value,

TABLE III
Arrhenius Parameters Determined by the Coats-Redfern Method [Eq. (4)] at 10 K/min

Models	E (kJ/mol)	$\ln A$ (min^{-1})	r^2
$A_{3/2}$	44.0	11.45	0.9880
A_2	31.4	7.47	0.9868
A_3	18.7	3.30	0.9841
A_4	12.3	1.07	0.9802
D_1	106.8	29.36	0.9981
D_2	124.3	35.00	0.9988
D_3	131.2	35.01	0.9958
D_4	122.2	32.12	0.9981
R_2	64.2	16.36	0.9975
R_3	67.8	17.11	0.9985
F_1	69.4	19.19	0.9889
P_2	21.7	4.06	0.9970
$n + m = 2; n = 1.5$	44.3	12.56	0.9473
$n + m = 2; n = 1.9$	85.2	24.61	0.9537
$n = 1.5$	81.6	23.16	0.9726
$n = 2$	95.4	27.62	0.9537
$n = 3$	127.2	37.77	0.9126

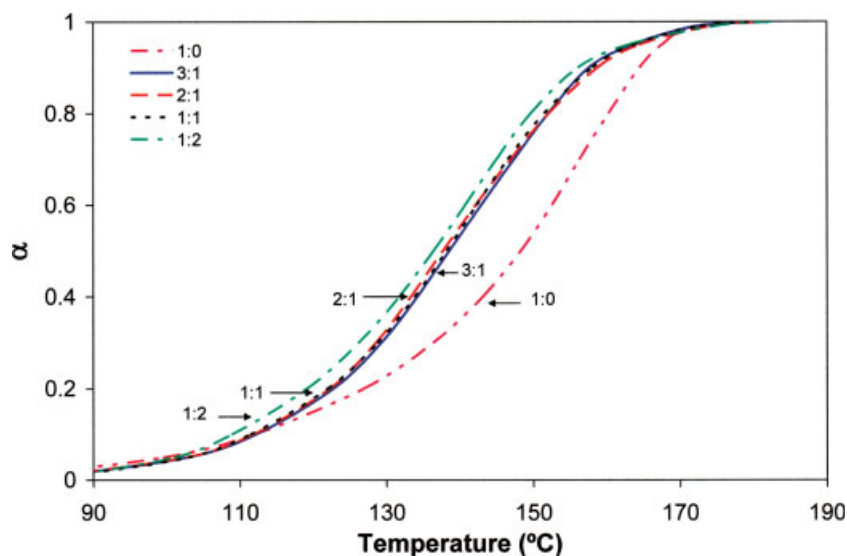


Figure 2 Conversion versus temperature at 15°C/min for different formulations.

T_{iso} , of 144°C.^{30,34} It is known that where there is an IKR between the activation parameters, a single mechanism describes the curing.³⁴ Furthermore, some authors maintain that if T_{iso} falls within the experimental range of temperatures, as is the case here, the kinetic model correctly describes the reaction process.³⁵ These considerations support the choice of the R_3 model as the one that best describes the curing process.

Table II also shows the experimental isothermal curing times and the curing times simulated using nonisothermal isoconversional data. The similarity of the two times indicates that we can simulate the isothermal curing reasonably well on the basis of nonisothermal data. This methodology can be useful for constructing TTT diagrams for the DGEBA/ γ -CL mixtures, since the isothermal curing of these systems is very fast and it cannot be tracked by means of DSC.

Figure 2 shows the α - T curves for all the formulations used at a rate of 15°C/min. It can be observed that with the increase in the γ -CL content the reaction speeded up and the curves were shifted to a lower temperature. In addition, this acceleration effect was practically independent of the amount of γ -CL present in the formulation and only in the 1 : 2 formulation did the α - T curve appear at slightly lower temperatures. This result suggests that the acceleration does not occur due to dilution of the reaction medium by the γ -CL, but rather due to the formation of some initiator species that are more active, owing to coordination of the initiator with the γ -CL. Using FTIR in a previous work,⁵ it was observed that the ytterbium triflate can coordinate with both the epoxy groups and the lactone, both

those types of coordination playing a part in initiation of the curing process.

Using the same methodology as in the case of the 1 : 0 formulation, the model that best reproduced the curing of all the formulations was R_3 . We determined the kinetic parameters using this model and the isoconversional methodology. Table IV shows these parameters for the formulations with γ -CL, while Table II shows the results for the pure resin analyzed previously. In all the formulations E increased with conversion and its values did not clearly show the accelerating effect of the γ -CL. As already explained, due to the compensation effect the kinetic changes are reflected best in the value of k . For conversions of over 0.1, all the formulations with γ -CL showed values for $k_{140^\circ\text{C}}$ that were higher than with the pure resin (formulation 1 : 0). In general, the 3 : 1, 2 : 1, and 1 : 1 formulations had values that were similar to $k_{140^\circ\text{C}}$, while the 1 : 2 formulation showed slightly higher value. These kinetic results are consistent with the experimental α - T curves shown in Figure 2.

It was also observed that there was a single IKR with $T_{iso} = 133^\circ\text{C}$ that grouped all the data for E and $\ln A$ for all the formulations with γ -CL, while the data for the pure resin were grouped in a slightly different IKR. This result suggests that with the addition of γ -CL, even in only a small amount, the curing mechanism is modified, possibly due to the formation of more active initiator species that are not found in the pure resin. These species condition the curing mechanism, which can be considered as a single mechanism that is common to all the formulations with γ -CL, although slightly different from that of the pure resin.

TABLE IV
Kinetic Parameters of Curing for Different Formulations^a

α	DGEBA/ γ -CL 3 : 1				DGEBA/ γ -CL 2 : 1				DGEBA/ γ -CL 1 : 1				DGEBA/ γ -CL 1 : 2			
	E (kJ/mol)	$\ln A$ (min ⁻¹)	$k_{140^\circ\text{C}}$ (min ⁻¹)	r^2	E (kJ/mol)	$\ln A$ (min ⁻¹)	$k_{140^\circ\text{C}}$ (min ⁻¹)	r^2	E (kJ/mol)	$\ln A$ (min ⁻¹)	$k_{140^\circ\text{C}}$ (min ⁻¹)	r^2	E (kJ/mol)	$\ln A$ (min ⁻¹)	$k_{140^\circ\text{C}}$ (min ⁻¹)	r^2
0.05	70.3	18.39	0.1256	0.9852	63.7	16.09	0.0842	0.9974	66.7	17.11	0.0978	0.9989	65.5	16.78	0.1015	0.9900
0.1	68.3	17.77	0.1213	1.0000	65.4	16.83	0.1083	0.9986	68.2	17.78	0.1249	0.9992	68.3	17.95	0.1446	0.9943
0.2	67.7	17.70	0.1332	1.0000	63.8	16.44	0.1184	0.9990	68.1	17.87	0.1392	0.9997	70.4	18.75	0.1743	0.9980
0.3	66.0	17.26	0.1389	1.0000	61.6	15.88	0.1261	0.9991	66.8	17.52	0.1444	0.9999	71.1	19.02	0.1841	0.9993
0.4	65.9	17.30	0.1488	0.9999	62.0	16.11	0.1413	0.9994	66.2	17.40	0.1521	0.9999	71.6	19.18	0.1894	0.9997
0.5	68.0	17.97	0.1611	0.9998	65.1	17.13	0.1609	0.9999	66.5	17.55	0.1609	0.9999	72.1	19.36	0.1930	0.9999
0.6	70.6	18.78	0.1682	0.9997	69.1	18.39	0.1756	0.9991	67.4	17.85	0.1679	0.9999	73.1	19.66	0.1956	0.9999
0.7	72.9	19.46	0.1695	0.9996	72.6	19.44	0.1805	0.9972	68.7	18.25	0.1713	1.0000	74.7	20.13	0.1966	0.9999
0.8	75.9	20.32	0.1679	0.9995	75.5	20.27	0.1765	0.9951	70.8	18.83	0.1691	1.0000	77.7	20.98	0.1939	0.9999
0.9	80.3	21.56	0.1612	0.9993	78.1	20.92	0.1615	0.9924	75.9	20.24	0.1564	1.0000	88.7	24.10	0.1764	1.0000
0.95	82.7	22.23	0.1562	0.9995	77.0	20.47	0.1437	0.9867	86.6	23.22	0.1339	0.9992	107.9	29.28	0.1177	0.9961

^a Kinetic parameters calculated in a similar way that kinetic parameters for formulation DGEBA/ γ -CL 1 : 0 collected in Table II using model R₃.

The acceleration effect exercised by the γ -CL on the curing process has already been observed in other epoxy/lactone systems using different lanthanide triflates as the initiator.^{5,6,14,15,30}

As already explained, we determined α_{gel} by means of nonisothermal TMA and DSC tests. As an example, Figure 3 shows the calculation method for the 1 : 1 formulation at 5°C/min. The materials were cured dynamically in TMA and DSC and the derivative curves length- T and α - T overlap. When the material was observed to gel in TMA (reduction of amplitude of oscillations by 95%), the calorimetric conversion was determined. This TMA methodology has already provided good results in the determination of the T_g of different materials.^{36,37} In this case, an increase in the amplitude of the oscillations was observed when T_g was passed. The TMA methodology presented in this study should be seen as being generally applicable to the determination of transitions where the mechanical stability of the materials changes.

Table V shows the experimental values for conversion at gelation, $\alpha_{\text{gel}}^{\text{exp}}$. Testing of loss of solubility gave similar results. With the increase in the γ -CL content, the material gelled at higher conversions. This result involved a reduction of contraction after gelation, since there was less groups to react during this phase of the curing. The formation of the SOE prior to gelation and the reaction of most of the SOE after gelation also resulted in a reduction of contraction after gelation.¹ Therefore, we can conclude that there are two ways of reducing contraction after gelation. One consists in changing the value of α_{gel} and the other consists in the polymerization of some expandable monomer after gelation.

The theoretical values of conversion at gelation $\alpha_{\text{gel}}^{\text{theor}}$ were determined using Flory's classic expression:³⁸

$$\alpha_{\text{gel}}^{\text{theor}} = \frac{1}{(f-1)^{1/2}} \quad (5)$$

where f is the functionality of the branching unit and it was calculated taking into account the molar composition of the mixture and the fact that the functionality of the pure DGEBA is 4 that of the γ -CL is 2.³⁹ The theoretical conversions showed the same trend as the experimental ones. In general, the formulations that are rich in DGEBA showed values of $\alpha_{\text{gel}}^{\text{theor}}$ that are higher than the experimental values, while just the opposite occurred with high proportions of γ -CL (formulation 1 : 2). It is known that many real formulations give conversions that are higher or lower than those predicted by Eq. (5) due to intramolecular cycling, reduction of the effective functionality of the system if chain ends increase, and the unequal reactivity of all the functional groups of the same type.^{31,40} In our case, the

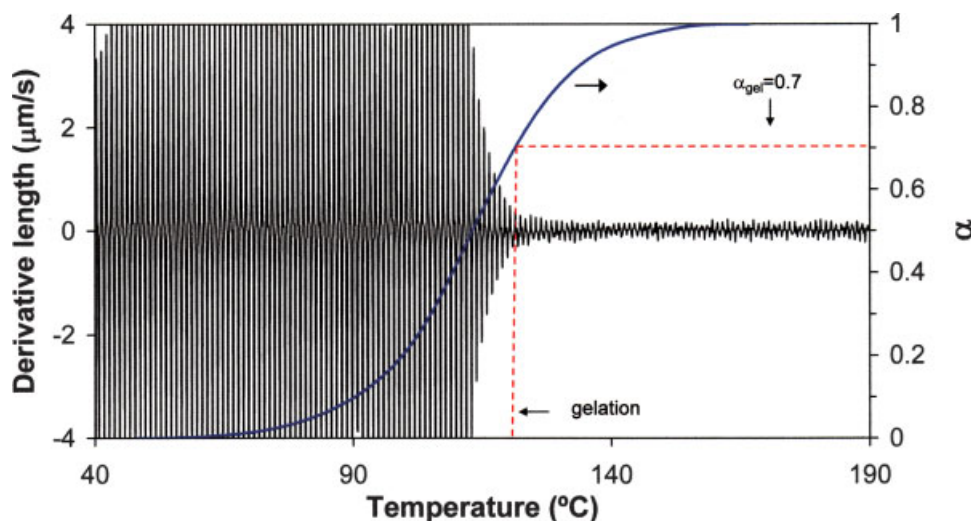


Figure 3 TMA thermogram (derivative length- T) and DSC thermogram (α - T) of nonisothermal of the DGEBA/ γ -CL 1 : 1 at 5°C/min. Determination of gelation.

formation of SOE that subsequently polymerized could also contribute to the differences observed. Matejka et al.³¹ found α_{gel} values between 0.2 and 0.45 for the DGEBA/ γ -butyrolactone system with small amounts of lactone. They observed that α_{gel} rises with an increase in the content of lactone and initiator.

To establish the structure-properties relationship and build TTT diagrams, our first step was to determine the T_g - α relationship on the basis of partially cured samples. The variation found in T_g during the curing process is due to two effects: the degree of crosslinking and the composition of the copolymer formed during the curing process. There are various theoretical approaches to the effect of crosslinking on T_g , one of the most widely accepted being that proposed by Nielsen and Dibenedetto:^{41,42}

$$\frac{T_g - T_{g0}}{T_{g0}} = \frac{\left(\frac{\varepsilon_x}{\varepsilon_M} - \frac{F_x}{F_M}\right) \alpha}{1 - \left(1 - \frac{F_x}{F_M}\right) \alpha} \quad (6)$$

where T_{g0} is the glass transition temperature of the system with the same chemical composition as the crosslinked polymer at $\alpha = 0$. If T_{g0} is taken as a constant, Eq. (6) predicts only the effect of the crosslinking. $\varepsilon_x/\varepsilon_M$ is the relationship between the lattice

energy of the crosslinked and uncrosslinked polymers and F_x/F_M is the corresponding ratio of segmental mobilities. These two relationships are generally treated as two characteristic empirical constants for each thermosetting system.

Equation (6) can be modified if we take into account that $T_g = T_{g\infty}$ at $\alpha = 1$:⁴³

$$\frac{T_g - T_{g0}}{T_{g\infty} - T_{g0}} = \frac{\frac{F_x}{F_M} \alpha}{1 - \left(1 - \frac{F_x}{F_M}\right) \alpha} \quad (7)$$

in this case F_x/F_M must be considered an adjustable parameter between 0 and 1.

Accepting the adaptation of Coachman's theory for chemical solutions to a thermosetting polymer carried out by Pascault and Williams⁴³ as correct, Eq. (7) can be expressed as:^{16,44}

$$\frac{T_g - T_{g0}}{T_{g\infty} - T_{g0}} = \frac{\frac{\Delta C_{p\infty}}{\Delta C_{p0}} \alpha}{1 - \left(1 - \frac{\Delta C_{p\infty}}{\Delta C_{p0}}\right) \alpha} \quad (8)$$

where $\Delta C_{p\infty}$ and ΔC_{p0} are the differences in heat capacity of crosslinked and uncrosslinked thermosets, respectively. Equations (7) and (8) are the same when $F_x/F_M = \Delta C_{p\infty}/\Delta C_{p0}$.

Figure 4 shows the T_g - α relationships for the 1 : 0 and 1 : 1 formulations, along with the fits obtained using Eqs. (6) and (7). It can be observed that both formulations correctly fit the two theoretical models and only small differences are found at high conversions. The lactone-rich system showed lower values for T_g throughout the curing process, since the lactone has lower functionality and produces a lattice with less crosslinking. Table VI shows the parameters relating to the T_g - α relationship. The higher

TABLE V
Functionality, Experimental α_{gel} , and Theoretical α_{gel}

Formulations	$\alpha_{\text{gel}}^{\text{exp}}$	$\alpha_{\text{gel}}^{\text{theor}}$	f
DGEBA/ γ -CL 1 : 0	0.30	0.58	4.00
DGEBA/ γ -CL 3 : 1	0.41	0.63	3.50
DGEBA/ γ -CL 2 : 1	0.49	0.65	3.33
DGEBA/ γ -CL 1 : 1	0.70	0.70	3.00
DGEBA/ γ -CL 1 : 2	0.88	0.77	2.66

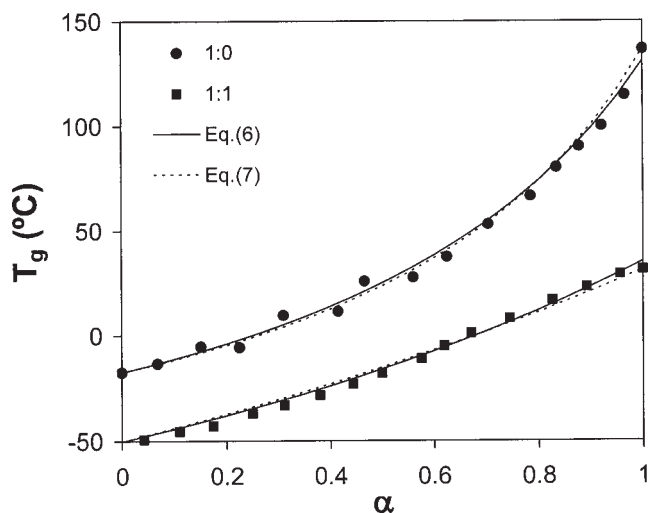


Figure 4 T_g against curing degree for the curing of the mixtures DGEBA/ γ -CL 1 : 0 and 1 : 1. Computed fits using eqs. (6) and (7).

values for F_x/F_M for the 1 : 1 formulation are consistent with the greater segmental mobility of a lattice with less crosslinking. When the material is crosslinked, ΔC_p decreases. This decrease has already been observed in other thermosetting materials.^{16,43,45} An increase in the density of the crosslinking gives rise to an increase in the stiffness of the chains and consequently in T_g . This stiffness involves a lower configurational entropy that can cause a reduction of ΔC_p .^{45,46} The experimental values for $\Delta C_{p\infty}/\Delta C_{p0}$ are close to those obtained by fitting F_x/F_M . This means that the hypotheses made in the deduction of Eq. (8) are correct, and this equation can be used to obtain the T - α relationship. In this case, all that needs to be known are the values of $\Delta C_{p\infty}$, ΔC_{p0} , $T_{g\infty}$, and T_{g0} , which can be determined experimentally on the basis of just two dynamic tests. This methodology [Eq. (8)] provides substantial time savings in comparison with the conventional methodology, based on scans of partially cured samples.

The TTT diagrams for the DGEBA/ γ -CL formulations were constructed using the experimental data determined previously, following the methodology set out below. The isoconversional lines were traced in the TTT diagram using Eq. (3) and nonisothermal kinetic parameters obtained at different conversions (Tables II and IV). T_{g0} and $T_{g\infty}$ were determined by

calorimetry of uncured and fully cured samples. Since gelation is an isoconversional effect, the gelation lines were drawn using Eq. (3) applied to the conversion α_{gel} determined using TMA and DSC (Table V). Vitrification times were taken as the times needed for the material to reach the conversion at which T_g is equal to the curing temperature, T_c . These times were calculated on the basis of the isoconversional lines as the time needed for a given conversion for T_c to equal T_g , corresponding to that conversion in the T_g - α relationship [Eq. (6) and Table VI]. The temperature at which the material gels and vitrifies simultaneously, $_{gel}T_g$, was determined as the temperature at which the material vitrifies with a conversion equal to α_{gel} [Eq. (6) and Table VI]. The time needed for the material to gel and vitrify simultaneously was determined by extrapolating the isoconversional line of α_{gel} to a curing temperature equal to $_{gel}T_g$.

Figures 5 and 6 show the TTT diagrams for the 1 : 0 and 1 : 1 formulations, respectively. These diagrams provide us with information on the curing times needed to attain a given degree of conversion and for the material to gel and/or vitrify. The material cannot cure below T_{g0} , so this would be an optimum temperature for storage. Between T_{g0} and $_{gel}T_g$, the liquid resin reacts until its T_g coincides with the curing temperature, at which point the material vitrifies and the reaction becomes controlled by diffusion. In this region, the material does not gel. Between $_{gel}T_g$ and $T_{g\infty}$, the material first gels and then vitrifies. Above $T_{g\infty}$, the material reacts completely and remains in the rubbery state after gelling.

The addition of lactone significantly changes the TTT diagram of the curing process. With large amounts of γ -CL curing times are substantially reduced. The 1 : 0 formulation requires high curing temperatures, above 137°C, to cure completely and keep the material from vitrifying. At lower temperatures complete curing cannot be guaranteed, unless a postcuring process is carried out at high temperature. On the other hand, the 1 : 1 formulation can cure completely without vitrifying at a temperature above 31°C ($T_c > T_{g\infty}$). The addition of γ -CL therefore makes it possible to reduce the curing temperature, which can involve the appearance of few thermal stresses as well as substantial energy

TABLE VI
Parameters Associated to the T_g - α Relationships

Formulations	T_{g0} (°C)	$T_{g\infty}$ (°C)	$\varepsilon_x/\varepsilon_M^a$	F_x/F_M^a	F_x/F_M^b	ΔC_{p0} (J g ⁻¹ K ⁻¹)	$\Delta C_{p\infty}$ (J g ⁻¹ K ⁻¹)	$\Delta C_{p\infty}/\Delta C_{p0}$
DGEBA/ γ -CL 1 : 0	-17	137	0.629	0.398	0.368	0.543	0.206	0.379
DGEBA/ γ -CL 1 : 1	-50	31	0.923	0.698	0.739	0.565	0.410	0.725

^a $\varepsilon_x/\varepsilon_M$ and F_x/F_M determined using eq. (6).

^b F_x/F_M determined using eq. (7).

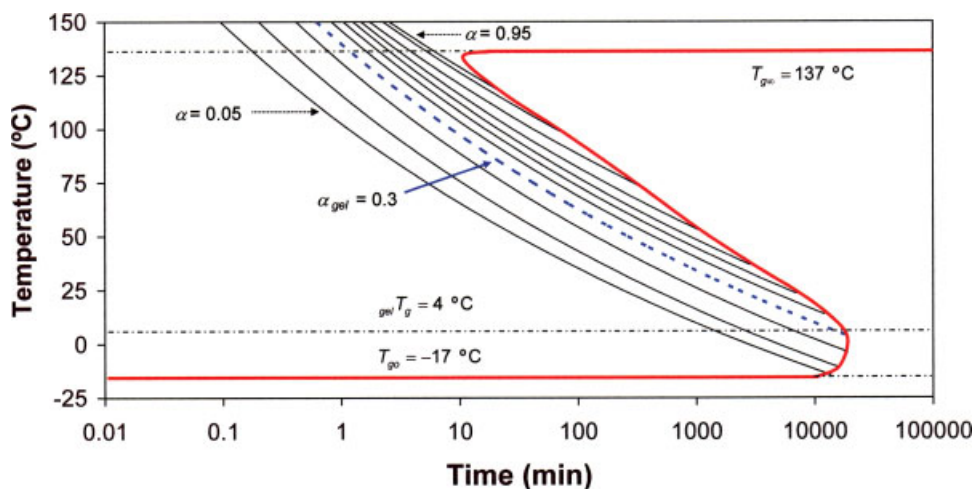


Figure 5 TTT diagram for the curing of the mixture DGEBA/ γ -CL 1 : 0. Vitrification curve (—), gelification curve (----). Isoconversional lines (0.05, 0.1, 0.2, 0.3, 0.4, 0.5, 0.6, 0.7, 0.8, 0.9, 0.95). T_{g0} , T_g , and $_{gel}T_g$ are also indicated.

savings. With an increase in the content of γ -CL, gelation occurs at higher conversions, giving rise to a reduction of the internal stresses in the gelled material. With the 1 : 1 formulation (Fig. 6), at temperatures near complete curing the vitrification line shows a certain delay, possibly related to the polymerization of SOE groups during the final phase of curing.^{1,5}

CONCLUSIONS

We studied the curing of mixtures in different proportions of DGEBA with γ -CL initiated cationically with ytterbium triflate using nonisothermal DSC and TMA experiments, with results equivalent to the isothermal experiments. Although there are a number of reactive processes involved in curing, it can be treated overall as a single kinetic process.

The curing kinetic was established by means of integral isoconversional analysis. Gelation was determined using a new methodology, by means of combined testing in TMA and DSC. Vitrification times were calculated on the basis of the T_g - α relationship and the isoconversional lines, with the assumption that the material vitrifies when T_g coincides with the curing temperature. The T_g - α relationship can be established on the basis of the residual curing of partially cured samples or on the basis of the ΔC_p of the cured and uncured material, determined in a nonisothermal test.

The curing processes of the DGEBA/ γ -CL systems are presented in the form of TTT diagrams that can be used to establish the optimum conditions for curing. The methodology used for these systems is applicable generally and can be used for the curing of other thermoset systems.

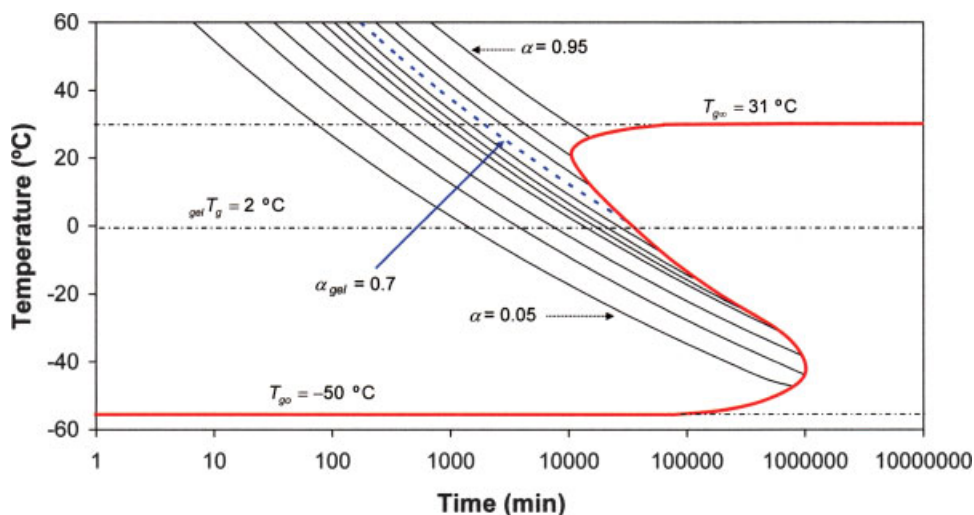


Figure 6 TTT diagram for the curing of the mixture DGEBA/ γ -CL 1 : 1. Vitrification curve (—), gelification curve (----). Isoconversional lines (0.05, 0.1, 0.2, 0.3, 0.4, 0.5, 0.6, 0.7, 0.8, 0.9, 0.95). T_{g0} , T_g , and $_{gel}T_g$ are also indicated.

The addition of γ -CL accelerates curing and reduces T_g . This allows energy savings, since the materials require less time and/or lower temperatures to cure completely. The formulations rich in γ -CL gel at higher α_{gel} . In this way, we are able to reduce the contraction that occurs subsequent to gelation and therefore also the internal stresses.

References

1. González, S.; Fernández-Francos, X.; Salla, J. M.; Serra, A.; Mantecón, A.; Ramis, X. *J Polym Sci Part A: Polym Chem*, to appear.
2. Sadhir, R. K.; Luck, M. R., Eds. *Expanding Monomers: Synthesis, Characterization and Applications*; CRC Press: Boca Raton, FL, 1992.
3. Bailey, W. J.; Sun, R. L.-J.; Katsuki, T.; Endo, H.; Iwama, H.; Tsushima, R.; Saigou, K.; Bitritto, M. M. In *Ring-Opening Polymerization*, ACS Symposium Series, Vol. 59; Saegusa, T., Goethals, E., Eds.; American Chemical Society: Washington, DC, 1977.
4. Ivin, K. J.; Saegusa, T., Eds. *Ring-Opening Polymerization*, Vol. 1; Elsevier Applied Science: London, 1984.
5. Mas, C.; Ramis, X.; Salla, J. M.; Mantecón, A.; Serra, A. *J Polym Sci Part A: Polym Chem* 2003, 41, 2794.
6. Jiménez, R.; Fernández-Francos, X.; Salla, J. M.; Serra, A.; Mantecón, A.; Ramis, X. *Polymer* 2005, 46, 10637.
7. Cervellera, R.; Ramis, X.; Salla, J. M.; Mantecón, A.; Serra, A. *J Polym Sci Part A: Polym Chem* 2005, 43, 5799.
8. Buchwalter, S. L.; Kosbar, L. L. *J Polym Sci Part A: Polym Chem* 1996, 34, 249.
9. Yang, S.; Chen, J.-S.; Körner, H.; Breiner, T.; Ober, C. K. *Chem Mater* 1998, 10, 1475.
10. Shimbo, M.; Ochi, M.; Inamura, T.; Inoue, M. *J Mater Sci* 1985, 20, 2965.
11. Matejka, L.; Dusek, K.; Chabanne, P.; Pascault, P. *J Polym Sci Part A: Polym Chem* 1997, 35, 665.
12. Yevstropov, A. A.; Lebedev, B. V.; Kiparariso, Y. G.; Alekseyev, V. A.; Stashina, G. A. *Vysokomol Soedin Ser* 1980, A22, 2450.
13. Mas, C.; Mantecón, A.; Serra, A.; Ramis, X.; Salla, J. M. *J Polym Sci Part A: Polym Chem* 2004, 42, 3782.
14. Mas, C.; Mantecón, A.; Serra, A.; Ramis, X.; Salla, J. M. *J Polym Sci Part A: Polym Chem* 2005, 43, 2337.
15. Fernández, X.; Salla, J. M.; Serra, A.; Mantecón, A.; Ramis, X. *J Polym Sci Part A: Polym Chem* 2005, 43, 3421.
16. Ramis, X.; Salla, J. M. *J Polym Sci Part B: Polym Phys* 1997, 35, 371.
17. Montserrat, S. *J Appl Polym Sci* 1992, 44, 545.
18. Montserrat, S. *Thermochim Acta* 1999, 330, 189.
19. Wisanrakkit, G.; Gillham, J. K. In *Polymer Characterization*, ACS Advanced Chemical Series; Craver, C. D.; Provder, T., Eds.; American Chem Society, Vol. 227: Washington, 1990; p 143.
20. Hofmann, K.; Glasser, W. G. *Thermochim Acta* 1990, 166, 169.
21. Enns, J. B.; Gillham, J. K. *J Appl Polym Sci* 1983, 28, 2567.
22. Vyazovkin, S.; Wight, C. A. *Annu Rev Phys Chem* 1997, 48, 125.
23. Coats, A. W.; Redfern, J. P. *Nature* 1964, 201, 68.
24. Kissinger, H. E. *Anal Chem* 1957, 29, 1702.
25. Ozawa, T. *Bull Chem Soc Jpn* 1965, 38, 1881.
26. Ramis, X.; Salla, J. M.; Puiggali, J. *J Polym Sci Part A: Polym Chem* 2005, 43, 1166.
27. García, S. J.; Ramis, X.; Serra, A.; Suay, J. *J Therm Anal Cal* 2006, 83, 429.
28. Ramis, X.; Salla, J. M.; Cadenato, A.; Morancho, J. M. *J Therm Anal Cal* 2003, 72, 707.
29. Cadenato, A.; Morancho, J. M.; Fernández-Francos, X.; Salla, J. M.; Ramis, X. *J Therm Anal Cal*, to appear.
30. Fernandez, X.; Ramis, X.; Salla, J. M. *Thermochim Acta* 2005, 438, 144.
31. Matejka, L.; Chabanne, P.; Tighzert, L.; Pascault, P. *J Polym Sci Part A: Polym Chem* 1994, 32, 1447.
32. Fernández-Francos, X.; Salla, J. M.; Cadenato, A.; Morancho, J. M.; Mantecón, A.; Serra, A.; Ramis, X. *J Polym Sci Part A: Polym Chem* 2007, 45, 16.
33. García, S. J.; Serra, A.; Ramis, X.; Suay, J. *J Therm Anal Cal*, to appear.
34. Vyazovkin, S.; Linert, W. *Int Rev Phys Chem* 1995, 14, 355.
35. Vyazovkin, S.; Linert, W. *Chem Phys* 1995, 193, 109.
36. Ramis, X.; Cadenato, A.; Morancho, J. M.; Salla, J. M. *Polymer* 2007, 48, 44.
37. Lucas, J. C.; Borrajo, J.; Williams, R. J. *J. Polymer* 1993, 34, 3216.
38. Flory, P. J. *Principles of Polymer Chemistry*; Cornell University Press: Ithaca, 1953; p 347.
39. Barton, J. M.; Hamerton, I.; Howlin, B. J.; Jones, J. R.; Liu, S. *Polym Int* 1996, 41, 159.
40. Odian, G. *Principles of Polymerization*, 3rd ed.; Wiley-Interscience: New York, 1991; p 108.
41. Nielsen, L. E. *J Macromol Sci Macromol Chem* 1969, C3(1), 69.
42. Dibenedetto, A. T. *J Polym Sci Part B: Polym Phys* 1987, 25, 25.
43. Pascault, J. P.; Williams, R. J. *J Polym Sci Part B: Polym Phys* 1990, 28, 85.
44. Couchman, P. R. *Macromolecules* 1987, 20, 1712.
45. Montserrat, S. *Polymer* 1995, 36, 435.
46. Gibbs, J. H.; DiMarzio, E. A. *J Chem Phys* 1958, 28, 373.